NASA Contractor Report 165979

ATTITUDE AND VIBRATION CONTROL OF A LARGE
FLEXIBLE SPACE-BASED ANTENNA

S. M. Joshi

NASA

National Aeronautics and
Space Administration

Langley Research Center
Hampton, Virginia 23665

ATTITUDE AND VIBRATION CONTROL OF A LARGE
FLEXIBLE SPACE- BASED ANTENNA

S. M. Joshi _____

SUMMARY

The problem of control systems synthesis is considered for controlling the rigid-body attitude and elastic motion of a large deployable space-based antenna. Two methods for control systems synthesis are considered. The first method utilizes the stability and robustness properties of the controller consisting of torque actuators and collocated attitude and rate sensors. The second method is based on the linear-quadratic-Gaussian (LQG) control theory. A combination of the two methods, which results in a two-level hierarchical control system, is also briefly discussed. The performance of the controllers is analyzed by computing the variances of pointing errors, feed misalignment errors and surface contour errors in the presence of sensor and actuator noise.

INTRODUCTION

The successful operation of the NASA space transportation system (STS) has opened a new era for more cost-effective utilization of space. One class of examples of future missions using the STS includes personal communication systems, Earth observation systems, radio astronomy systems, and electronic mail systems. These missions require large space-based antennas. For early missions utilizing large antennas, the development of a deployable antenna which can be transported into orbit using a single shuttle flight has a special appeal. The 122 meter hoop/column antenna represents such a concept for relatively near-term missions.

The detailed description of a technology development program for large space-based antennas was presented in Ref. 1. The hoop/column antenna concept, shown in figure 1, consists of a deployable central mast attached to a deployable hoop by cables held in tension. A secondary drawing surface is used to produce the desired contour of the radio-frequency (RF) reflective mesh. The RF surface shaping is accomplished by mesh shaping ties. The deployable mast contains a number of telescoping sections which are deployed by means of a cable drive system. The hoop consists of 48 rigid segments, and is deployed by four motor drive units. The reflective mesh is made of knit gold-plated molybdenum wire, and is attached to the hoop by quartz or graphite fibers. The RF mesh is shaped in the desired manner (e.g. parabolic or spherical) with control cords attached to the mesh through the secondary drawing surface.

In order to achieve the required RF performance, the antenna must be controlled to specified precision in attitude and shape. For example, for missions such as the land mobile satellite system (LMSS), which is a communications concept for providing mobile telephone service to users in the continental United States, it is necessary to achieve a pointing accuracy of 0.03 degree RMS (root mean square) and a surface accuracy of 6 mm RMS. It is also necessary to have stringent control (usually a fraction of a degree) on the motion of the feed (located near one end of the mast) relative to the mesh. In this paper, two approaches are considered for control systems synthesis for such an antenna. The first approach uses a "collocated" controller, which consists of torque actuators and collocated attitude and rate sensors The second approach is based on the linear-quadratic-Gaussian (LQG) control theory. The performance of the controllers is evaluated in the presence of sensor and actuator noise.

HOOP/COLUMN ANTENNA MATHEMATICAL MODEL

A large space structure (LSS) such as the hoop/column antenna has, in theory, infinite number of structural modes. In order to facilitate analytical treatment, it is necessary to have a finite order "evaluation" model which is an acceptable representation of the LSS. The evaluation model considered in this paper is a 20 structural mode, finite element model of the 122 meter diameter hoop/column antenna as described in ref. 2. For the purpose of this study, four, 3-axis torque actuators (a total of 12 actuators) are assumed to be located on the mast at points shown in figure 2. In addition to 20 structural modes, three rigid-body rotations are also included. The equations of motion are given by:

$$I_s \ddot{\alpha}_s = \sum_{j=1}^{n_T} T_j \tag{1}$$

$$\ddot{q} + \dot{D}q + \Lambda q = \Phi^T T \tag{2}$$

where I_s is the 3 by 3 inertia matrix, n_T is the number of 3-axis torque actuators, $\alpha_s = (\phi_s, \theta_s, \psi_s)^T$, denotes the rigid-body attitude vector, T_j denotes the 3×1 torque vector produced by the jth (3-axis) torque actuator, q is the $n_q \times 1$ modal amplitude vector (for n_q structural modes), $D = D^T \geq 0$ is the matrix representing the inherent damping.

$$\Lambda = \text{diag.} (\omega_1^2, \omega_2^2, \ldots, \omega_{nq}^2) \tag{3}$$

where ω_i is the natural frequency of the ith structural mode.

$$\phi^T = [\phi_1{}^T \; \phi_2{}^T \ldots \phi_{nT}{}^T] \tag{4}$$

Φ^T is the $n_q \times 3n_T$ matrix of "mode slopes", and Φ_j^T corresponds to the $n_q \times 3$ mode slope matrix for the location of the jth torque actuator. The $3n_T \times 1$ vector T is given by

$$T = [T_1{}^T, T_2{}^T, \ldots, T_{nT}{}^T]^T \tag{5}$$

The total attitude vector (including the contributions of the rigid-body and structural modes) at the location of the jth actuator is given by

$$y_{\alpha j} = \alpha_s + \phi_j q \tag{6}$$

The data presented in the model consists of structural frequencies, , three mode shapes and three mode slopes (6 degrees of freedom) at 6 points on the mast, at 8 points corresponding to the feeds, feed panels., etc., and at two points corresponding to the at two solar panels. Three mode shapes (3 degrees of freedom) at 96 points corresponding to the mesh surface are also given. The knowledge of the mode-shapes enables one to co pute the elastic displacements (X, Y, Z directions), and that of the mode slopes enables one to compute the elastic rotations (about X,Y,Z axes), from a given modal amplitude vector q. Table I shows the mass and inertia properties of the hoop/column antenna, and the frequencies of the first 20 structural modes are given in Table II. Figure 3 shows the plots of elastic deformations resulting from some of the modes. (The first and the sixth modes are torsion modes, and are not shown because they have very small translational deformations.) The assumed nominal damping ratio of 1 per cent (0.01) will be used in this paper for the numerical computations.

CONTROL SYSTEMS DESIGN

As stated previously, only torque actuators located on the mast are considered in this paper for controlling the antenna attitude and flexible motion. Because of the geometry of the antenna, it appears that reaction jets located on the hoop might be effective in controlling rigid-body roll and torsion modes; however, because of their propellant storage requirements and to avoid possible hardware-related difficulties in generating required precision

control forces, reaction jets are not considered in this preliminary investigation. As pointed out earlier, surface accuracy is of extreme importance to successful operation of the antenna. The surface can be actively controlled by pulling the control stringers; however, from practical considerations, it is preferable to avoid active surface control if at all possible, and to try to control the surface using only the torque actuators on the mast.

Two approaches are considered in this paper for control systems synthesis. The first approach requires collocated sensors and actuators, while the second approach is based on the LQG control theory.

Method I- Collocated Controller

It is assumed that n_T, 3-axis attitude and rate sensors are located on the mast at the locations of the torque actuators. The equations of motion are (from eqs. 1 and 2):

$$A_s \ddot{x}_s + B_s \dot{x}_s + C_s x_s = \Gamma^T T \tag{7}$$

where $A_s = \text{diag.} (I_s, \bar{I}_{nq \times nq})$,

$$x_s^T = (\alpha_s^T, q^T),$$

$B_s = \text{diag.} (0, D)$, $C_s = \text{diag.} (0, \Lambda)$,

$$\Gamma^T = [\Gamma_1^T, \Gamma_2^T, \ldots, \Gamma_{nT}^T]$$

where $\Gamma_j = [\bar{I}_{3 \times 3}, \Phi_j]$

($\bar{I}_{k \times k}$ denotes the k x k identity matrix.)

Since the attitude and rate sensors are collocated with torque actuators, the measured attitude and rate vectors are:

$$y_\alpha = \Gamma x_s + w_p \tag{8}$$

$$y_\omega = \Gamma \dot{x}_s + w_r \tag{9}$$

where y_α, y_ω are the $3n_r \times 1$ vectors of measured attitude and rate, and w_p, w_r are $3n_r \times 1$ sensor noise vectors. Consider the control law:

$$T = -K_p y_\alpha - K_r y_\omega \qquad (10)$$

where K_p and K_r denote $3n_r \times 3n_r$, symmetric proportional and rate gain matrices. The closed-loop equations, ignoring the noise terms, then become:

$$A_s \ddot{x}_s + \bar{B}_s \dot{x}_s + \bar{C}_s x_s = 0 \qquad (11)$$

where
$$\bar{B}_s = B_s + \Gamma^T K_r \Gamma \qquad (12)$$

$$\bar{C}_s = C_s + \Gamma^T K_p \Gamma \qquad (13)$$

It can be shown that the closed-loop system as given by Eq.(11) is stable in the sense of Lyapunov if $K_p > 0$ and $K_r \geq 0$, and is asymptotically stable if $K_p > 0$, $K_r > 0$, and the system is stabilizable (Ref. 3). This method attempts to make matrices $\bar{B}_s$ and $\bar{C}_s$ equal some desired matrices B_d and C_d. For example, in order to assign closed-loop damping ratio ρ_{di} to structural mode i without changing their frequencies, and to assign closed-loop damping ratio and frequency ρ_{si}, ω_{si} (i=x,y,z) to the rigid-body modes,

$$B_d = 2\,\mathrm{diag}(\rho_{sx}\omega_{sx}, \rho_{sy}\omega_{sy}, \rho_{sz}\omega_{sz}, \rho_{d_1}\omega_1, \ldots, \rho_{d_{nq}}\omega_{nq}) \qquad (14)$$

$$C_d = \mathrm{diag.}\ (\omega_{sx}^2, \omega_{sy}^2, \omega_{sz}^2, \omega_1^2, \omega_2^2, \ldots, \omega_{nq}^2) \qquad (15)$$

The equations to be solved for K_p and K_r then become

$$\Gamma^T K_r \Gamma = B_d - B_s \triangleq \bar{B}_d \qquad (16)$$

$$\Gamma^T K_p \Gamma = C_d - C_s \triangleq \bar{C}_d \qquad (17)$$

($\triangleq$ denotes equality by definition.) It will be assumed that Γ^T is of full rank, or has been reduced to be of full rank (by eliminating locations corresponding to linearly dependent columns). If it is

5

desired to control only n_c ($\leq n_q+3$) modes, then the rows corresponding to the modes which are not controlled are assumed to be removed from Γ^T. It is also assumed that $\bar{B}_d$ and $\bar{C}_d$ are nonnegative definite. If the number of controlled modes, n_c, is less than or equal to the number of actuators, m (row dimension of Γ^T), then the solution

$$K_r = \Gamma(\Gamma^T\Gamma)^{-1}\bar{B}_d(\Gamma^T\Gamma)^{-1}\Gamma^T \qquad (18)$$

minimizes the Frobenius norm of K_r, where the Frobenius norm is defined as:

$$||K_r||_F = \left(\sum_i \sum_j K_{rij}^2\right)^{\frac{1}{2}}$$

For the case $n_c > m$, the solution which minimizes the Frobenius norm of the equation error in (16) is given by (Ref. 4)

$$K_r = (\Gamma\Gamma^T)^{-1}\ \Gamma\bar{B}_d\Gamma^T\ (\Gamma\Gamma^T)^{-1} \qquad (19)$$

The main advantage of this method is the guaranteed stability. The closed-loop system is stable in the sense of Lyapunov regardless of the number of modes in the model, and in spite of parameter inaccuracies (Ref. 4). This result is true only for perfect (i.e., linear, instantaneous) actuators and sensors; however, even with actuators and sensors of finite but sufficiently high bandwidth (Ref. 5), the closed-loop system would be stable.

In practice, it may be impossible to exactly collocate the actuators and sensors. The folowing analysis obtains a bound on the tolerable inaccuracy of collocation.

Let the closed-loop system of Eq. (11) be asymptotically stable (for perfect collocation).Then, given a 2nX2n matrix $Q=Q^T>0$, there exists a matrix $P=P^T \geq 0$ such that

$$A_c^T P + PA_c = -Q \qquad (20)$$

where A_c is the 2nX2n closed-loop system matrix corresponding to Eq. (11). Consider now the case where the sensors are not exactly collocated with the actuators. In this case, the sensor equations become (ignoring noise terms):

$$y_{\dot{\alpha}} = (\Gamma + \delta\Gamma_1) \; x_s \tag{21}$$

$$y_\omega = (\Gamma + \delta\Gamma_2) \; \dot{x}_s \tag{22}$$

where $\delta\Gamma_1 = [0, \delta\Phi_1]$ represents the collocation error for the attitude measurements and $\delta\Gamma_2 = [0, \delta\Phi_2]$ represents that for the rate measurements. The following theorem gives bounds on $\delta\Phi_1, \delta\Phi_2$ which ensure stability.

Theorem 1.- The closed-loop system with imprecisely collocated sensors and actuators is Lyapunov-stable if

$$||K_p||_s \, ||\delta\Phi_1||_s + ||K_r||_s \, ||\delta\Phi_2||_s \leq \frac{\lambda_m(Q) \; \lambda_m(A)}{2||\Gamma||_s \lambda_M(P)} \tag{23}$$

where $||L||_s$ denotes the spectral norm of a matrix L

$$||L||_s = (\text{Maximum eigenvalue of } L^T L)^{1/2}$$

$\lambda_m(\;)$ and $\lambda_M(\;)$ denote the smallest and largest eigenvalues.

Proof.- The closed-loop equation with collocation error can be written in the state variable form as:

$$\dot{z} = A_1 z - \begin{bmatrix} 0 & 0 \\ A^{-1}\Gamma^T K_p \delta\Gamma_1 & A^{-1}\Gamma^T K_r \delta\Gamma_2 \end{bmatrix} z \tag{24}$$

$$z = (x^T, \dot{x}^T)^T$$

Consider a Lyapunov function

$$V(z) = z^T P z \tag{25}$$

Then it can be shown that

$$\dot{V} = -z^T Q z + 2 \, z^T P E z \tag{26}$$

7

where E denotes the coefficient matrix in the second term on the right-hand-side of Eq. (24). For $\dot{V}$ to be nonpositive, the inequality

$$z^T PEz \leqq z^T Qz$$

should hold. But

$$z^T PEz \leq ||P||_s ||E||_s ||z||^2 \quad \text{and}$$

$$z^T Qz \geq \lambda_m(Q)||z||^2$$

Therefore, $\dot{V}$ is nonpositive if

$$||P||_s ||E||_s ||z||^2 \leq \tfrac{1}{2} \lambda_m(Q)||z||^2$$

or, since $||P||_s = \lambda_M(P)$

$$||E||_s \leq \frac{\lambda_m(Q)}{2\lambda_M(P)}$$

The inequality (23) can then be obtained by using the properties of the spectral norm to obtain an upper bound on $||E||_s$. It should be noted that a strict inequality in Eq.(23) assures asymptotic stability. The bound given by the theorem is conservative and difficult to compute. Also, it depends on the choice of Q, and requires the knowledge of the system parameters. Additional investigation is needed in this area in order to obtain less conservative bounds. However, it is apparent from the theorem that the system will be asymptotically stable for sufficiently small collocation errors.

Although the "collocated controller" approach has desirable stability and robustness properties, the decision regarding which modes to control rests with the designer, as does the choice of the desired matrices B_d and C_d. The most straightforward choices of B_d and C_d are given in Eqs.(14) and (15); however, this artificial decoupling may not give the best performance, and might result in unreasonably high gains. One method of systematically selecting these matrices for computing rate gains was given in Ref 6. However, the choice of the weighting matrix which is required in this metho was not discussed. The choice of B_d and C_d, which give the best

performance with the smallest possible magnitudes of the feedback gains, remains an open area of research.

Method II- Controller Based on LQG Theory

This approach uses the steady-state LQG control theory as a design tool. Unlike the collocated controller, the LQG controller does not automatically guarantee the closed-loop stability. This is because the plant (i.e., the LSS) has an infinite number of structural modes, and one can actively control only a finite number of modes via this approach. Furthermore, from practical cosiderations, in order to limit the number of feedback channels and the complexity of the controller, it is usually necessary to design a controller which is of much lower order than the "evaluation" model. (An evaluation model is an acceptably realistic representation of the LSS which consists of a finite but large number of structural modes.) The use of lower order controller may cause instability because of the (ref. 7) unwanted excitation of the residual or uncontrlled modes by the control input ("control spillover") and the unwanted contribution of the residual modes to the sensor outputs ("observation spillover"). It is well known that the LQG controller minimizes the performance index:

$$J_L = \lim_{t_f \to \infty} \frac{1}{t_f} \mathcal{E} \int_0^{t_f} (z^T \hat{Q} z + u^T R u) \, dt \tag{27}$$

where z, u denote the state and control vectors, $\hat{Q} = \hat{Q}^T \geq 0$, $R = R^T > 0$ denote the state and control weighting matrices, and $\mathcal{E}$ denotes the expected value operator. An LQG controller consists of a linear-quadratic(LQ) regulator in tandem with a state estimator (Kalman-Bucy filter). Only the steady-state versions of the LQ regulator and the Kalman-Bucy filter, which use time-invariant gains, are used in order to facilitate implementation. The Kalman-Bucy filter uses the knowledge of the system model (rigid-body modes and selected structural modes which are to be controlled) and the sensor outputs in order to generate an estimate of the state vector (i.e., an estimate of $a_s, q_c, \dot{a}_s$ and $\dot{q}_c$, where q_c denotes the modal amplitude vector of the controlled modes). This estimate is multiplied by the regulator gain matrix in order to synthesize the control torques. Thus the central problem in primary controller design is to ensure the stability of the full-order closed -loop system, which is not guaranteed because of the use of truncated models in regulator and estimator design. Several methods for primary controller design based on the LQG theory were discussed in Ref 8. They include i) truncation method, in which the residual modes are merely ignored in the design process, ii)modified truncation, or model error sensitivity suppression (MESS) method (Ref. 9) iii) use of higher order estimator iv) selective modal suppression, etc. Of these methods, the first two were found to be effective. Stability bounds

on spillover terms were obtained for this type of controllers in Ref 10.

The "Two-level" controller (Ref 11) is a variation of the LQG controller in which the collocated controller is also used, but only for damping enhancement. The controller consists of two hierarchical levels: i) a secondary controller, the function of which is to enhance damping in the LSS structural modes without attempting to control rigid-body modes, and ii) a primary controller for controlling the rigid-body modes and possibly some selected structural modes. Robust secondary control can be achieved using feedback of relative velocities (or angular velocities) between various points on the LSS. If the actuators and sensors for the secondary controller are collocated, the closed-loop system (excluding rigid-body modes) with only the secondary controller in the loop is guaranteed Lyapunov-stable with positive semidefinite rate gain ($K_r \geq 0$), and is asymptotically stable if $K_r > 0$, and if (Λ, Φ^T) is controllable (Ref 3). The closed-loop secondary system is stable regardless of the number of modes and parameter inaccuracies. In addition, under certain conditions, the system is asymptotically stable in the large (ASIL) for sector-type sensor and actuator nonlinearities. (Ref 5). A variation of the secondary controller is obtained by using one or more Annular Momentum Control Devices (AMCDs) as discussed in Ref. 3.

The procedure for secondary controller design using velocity feedback is similar to that for the collocated controller, the difference being that the first three rows of the Γ^T matrix are zero, and the rest of the rows consist of differences between the appropriate columns of Γ^T. Thus the secondary controller is used only to enhance the damping of the structural modes.

The closed-loop system including the secondary controller provides the starting point for the design of the primary controller. The primary controller design is accomplished using the LQG control theory as discussed previously. Since the damping of the LSS is enhanced by the secondary controller, it should facilitate the design of the primary controller such that the overall system has an acceptable degree of stability.

PERFORMANCE EVALUATION

The performance of the control system can be evaluated by computing the standard deviations or root mean square (RMS) values of various errors in the presence of sensor noise, actuator noise and other disturbances. Disturbances such as gravity gradient and solar pressure are low-frequency and predictable, and can be open-loop compensated. However, sensor and actuator noise represent very significant sources of error. In this paper, the attitude sensors

and rate sensors are assumed to have additive white measurement noise. The nominal standard-deviation intensities of these noise processes are assumed to be 0.488 arc-second and 0.031 arc-second/sec. respectively (Ref 12). The rate gyro drift is not modeled. The actuator noise is also assumed to be zero-mean and white. Since data were not available on nominal actuator noise, it was not included in the nominal performance computations. However, the actuator noise was included in the computation of the parametrized data (i.e., coeficient δa, as will be explained later). The sensor and actuator noises additively enter the closed-loop equations for both the controllers considered, and in both the primary and the secondary levels of the two-level controller. The final closed-loop equation is of the type:

$$\dot{x} = Ax + Bv \tag{28}$$

where x is the overall closed-loop state vector $(n_x \times 1)$, A is the strictly Hurwitz closed-loop matrix, B is the noise input matrix, and v is a vector white noise process whose entries represent all the noise terms. The closed-loop covariance evolves according to the equation

$$\dot{\Sigma} = A\Sigma + \Sigma A^T + BVB^T \tag{29}$$

where $\Sigma(t) = E[x(t)x^T(t)]$ is the covariance matrix, and V is the covariance intensity matrix of the noise process v. If v is a stationary process, Σ approaches a steady-state value $\bar{\Sigma}$ as t tends to infinity. Since the performance variables of interest (e.g. attitude angles and deflections at various points on the antenna) are linear transformations of the state vector x, the variances of these variables can be obtained by appropriate transformations of $\bar{\Sigma}$. A number of methods are available for numerical solution of the steady-state version of Eq. (29). The method given in Ref. (13) is used in this paper.

NUMERICAL RESULTS

As stated previously, four 3-axis torque actuators and four 3-axis attitude and rate sensors (at the same locations) are used for the nominal control systems design. Three types of zero-mean, white-noise disturbances are considered for performance analysis. Each attitude and rate sensor output is assumed to be contaminated with additive white measurement noise, and each actuator is assumed to introduce additive white noise. All individual noise processes are assumed to be mutually uncorrelated. The basic design objectives are: 1) to obtain sufficiently high bandwidth (i.e.,closed-loop

frequencies corresponding to rigid-body modes) and satisfactory closed-loop damping ratios for rigid-body and structural modes 2) to obtain satisfactory RMS pointing errors, feed motion errors, and surface errors. The first design objective arises from the need to obtain sufficiently fast error decay when a step disturbance (such as sudden thermal distortion caused by entering or leaving Earth's shadow) occurs. The second design objective arises from the RF performance requirements. These two objectives may not necessarily be compatiable, and may even be conflicting. For example, the use of increased feedback gains for obtaining higher bandwidths and damping ratios will, in general, result in higher RMS errors (because of the amplified effect of sensor noise) beyond a certain point. Therefore, it is necessary to carefully consider the tradeoffs between the speed of response and lower RMS errors.

As a part of the first design objective, the desired rigid-body closed-loop bandwidths in the range of 0.02- 0.25 rad/sec were considered. Also as a part of the first objective, the desired real parts of the closed-loop eigenvalues correesponding to the structural modes, $(\rho\omega)_d$ in the range 0- 0.5 were considered for the collocated controller (inherent damping of 1 % is assumed for all structural modes, and $(\rho\omega)_d$ =0 implies "no additional desired damping".). That is, the desired damping ratio for each structural mode was inversely proportional to its frequency, and the desired closed-loop eigenvalues would lie on- or to the left of the $-(\rho\omega)_d$ line in the complex plane. For the LQG controller, the weights corresponding to $\dot{q}$ can be successively increased in order to achieve successively higher damping on the structural modes. RMS errors were computed for nominal noise standard deviation intensities (as stated previously) for different values of the closed-loop rigid-body frequency ω_s (same for all three axes), and desired closed-loop structural damping. The desired rigid-body damping ratio ρ_s was held at 0.7. The five measures of performance considered were: a) maximum (taken over all points on the mast) RMS pointing errors $\epsilon_\phi, \epsilon_\theta, \epsilon_\psi$ about the X, Y, Z axes (all erors include the contributions of rigid body modes and all 20 structural modes). b) maximum RMS feed motion error (maximum taken over seven points corresponding to feeds and feed panels, with error at each point being defined as the resultant of X, Y, Z direction motions of each point relative to the point on the mast where the rellective surface intersects the mast). c) maximum RMS surface error (maximum taken over the resultant displacements from nominal positions , of 96 points on the surface).

The nominal performance of the collocated controller was first obtained. The closed-loop eigenvalues for the collocated controller indicated satisfactory stability margins (i.e., real parts close to the desired values). Figure 4 shows the nominal performance of the collocated controller for the different values of the closed-loop rigid-body frequency, ω_s= 0.02 rad/sec, 0.1 rad/sec and 0.25 rad/sec (same ω_s for the three axes, with damping ratio ρ_s =0.7) The nominal performance does not include actuator noise because of the present

lack of knowledge of the type of device that will be used. The nominal attitude and rate sensor noises are as stated previously. It is apparent from Fig. 4 that the RMS pointing errors $\epsilon_\phi, \epsilon_\theta, \epsilon_\psi$ decrease as $(\rho\omega)_d$ is increased. However, as ω_s is increased, the RMS pointing errors first decrease, and then increase. RMS feed motion and surface errors go through a minimum as $(\rho\omega)_d$ is increased. As can be seen from Fig. 4, the nominal RMS errors are very low, well below the allowable limits. For example, for $\omega_s = 0.1$ rad/sec and $(\rho\omega)_d = 0.25$, $\epsilon_\phi = 0.62 \times 10^{-3}$ degree, $\epsilon_\theta = 1.0 \times 10^{-5}$ degree, $\epsilon_\psi = 0.55 \times 10^{-3}$ degree, $\epsilon_f = 0.08$ mm, $\epsilon_s = 0.14$ mm, where $\epsilon_i (i = \phi, \theta, \psi, f, s)$ denote (maximum) three RMS pointing errors, RMS feed motion error, and RMS surface error respectively. For effectively designing a control system, more generic data will be helpful. Since the covariance intensities of the three noises considered (V_p, V_r, and V_a, which denote the attitude and rate sensor noise and the actuator noise) enter the covariance equation linearly, it is possible to parametrize the data by activating each noise one at a time. Figures 5, 6, and 7 show the coefficients $\delta_{pi}, \delta_{ri}, \delta_{ai}$ ($i = \phi, \theta, \psi, f, s$), which represent the appropriate error variance (denoted by subscript i), obtained by making each of the noises V_p, V_r and V_a equal to unity one at a time while the other two are being held at zero. As a result, any of the five performance measures ϵ_i ($i = \phi, \theta, \psi, f, s$) can be computed for any given set of actual noise variances as follows:

$$\epsilon_i = (\delta_{pi} V_p + \delta_{ri} V_r + \delta_{ai} V_a)^{1/2}$$

where the units of ϵ_i are degree for $i = \phi, \theta, \psi$, and mm for $i = f, s$. units of the noise variances are $(\text{rad})^2$, $(\text{rad/sec})^2$, and $(\text{ft-lb})^2$ respectively. The coefficients in Figs. 5-7 are plotted for three values of : 0.02, 0.1 and 0.25 rad/sec in order to consider three response speeds. Generic data such as these can provide useful guidelines for antenna control system design.

The nominal performance with the LQG- based controller was next obtained. In addition to the three rigid-body modes, it was arbitrarily decided to control the first three structural modes. The nominal desired values of ω_s were selected to be 0.02, 0.1 and 0.25 rad/sec, corresponding to slow, medium and fast response speeds ($\beta_s = 0.7$). The estimator was designed to estimate state variables corresponding only to those modes which were controlled in this preliminary analysis. With a little trial and error, it was straightforward to arrive at performance function weights Q which yield the desired ω_s and β_s for the LQ regulator. Instead of using the actual noise parameters for the design of the Kalman- Bucy filter, (which would give extremely slow filter response) weighting matrices were adjusted by trial and error to yield closed-loop frequencies (corresponding to rigid-body modes) approximately 3-4 times ω_s, with damping ratios = 0.7. Satisfactory (0.7 or better) damping ratios for the structural modes were obtained by adjusting

13

the corresponding weights. Keeping the estimator fixed for each ω_s, the weights on the modal velocities ($\dot{q}$) in the regulator design were increased by factor of 10 at each step, and nominal performance was computed similar to the collocated case. The closed-loop eigenvalues indicated satisfactory stability margins for the controlled modes. The closed-loop damping ratios for most of the residual modes changed very little (i.e., remained between 0.0075 and 0.013), while that for the rest of the residual modes increased. The nominal performance is plotted in Fig. 8 for ω_s =0.02, 0.1 and 0.25 rad/sec. The RMS errors are significantly lower than those for the collocated controller. At least for this preliminary model, the LQG method using simple modal truncation does not cause any appreciable destabilizing effect on the residual modes for the range of closed-loop bandwidth considered (0.02-0.5 rad/sec). Therefore, it is not necessary to use special techniques for the reduction of spillover (e.g. Ref. 8). The data for the LQG controller can also be parametrized in the same fashion as the collocated controller. The resulting coefficients are shown in Figs. 9-11. It can be seen that the coefficients δ_{pi} and δ_{ri} are much lower for the LQG controller than for the collocated controller, while δ_{ai} appears to be roughly the same. The LQG feedback gains were much smaller than those for the collocated controller (typically by a factor of 100 or more).

Generation of parametrized data such as these can provide useful guidelines for the antenna control systems design. In order to evaluate the controllers more completely, the following investigations were made:

Effect of imprecise collocation.- In order to investigate the effect of imprecise sensor/actuator collocation on the collocated controller, all sensors were displaced from the corresponding actuators by ±60 cm along the mast. For the nominal case (ω_s =0.1 rad/sec, $(pw)_H$ =0.25) the closed-loop eigenvalues remained practically unchanged, and RMS errors showed less than 1% increase.

Effect of using fewer actuators/sensors.- In order to investigate if fewer actuators/sensors can be used, both the designs were carried out for the nominal case, with a) one (3-axis) actuator and sensor (actuator no. 1 in Fig. 2) b)two actuators/sensors (nos. 1 and 3), and c)three actuators/sensors (nos. 1, 2 and 3). The collocated controller failed to meet the rigid-body bandwidth and damping ratio requirements with fewer than 4 actuators, while the LQG controller met the requirements with two or more actuators. The RMS performance of the LQG controller deteriorated by about 50% with 2 actuators (as compared to the nominal 4-actuator case), which was well within the acceptable bounds. the magnitudes of the maximum elements of the regulator and Kalman gain matrices increased by about 70% and 15% respectively, which is not excessively large. In view of this analysis, it appears that an acceptable LQG design may be obtained using only two actuators. It was not possible to obtain a satisfactory stable LQG design with a single actuator and sensor.

Effect of imprecise knowledge of parameters.- A change in parameters $(\omega_i \text{ and } \beta_i)$ of upto $\pm 10\%$ caused less than 2% deterioration in the collocated controller performance , and caused under 4% deterioration in the LQG controller performance.

Two-level controller.- A secondary collocated controller was first designed for the $(\beta\omega)_j$ =0 to 0.5 range. The primary LQG controller was then designed to obtain ω_s =0.1 rad/sec. However, this caused the RMS errors to increase by a factor of 10 or more as compared to the case with LQG controller alone.

Effect of number of modes controlled.- For the LQG controller, the number of modes controlled (and estimated) was varied from n_c=3 (rigid-body only) to 9 (rigid-body and the first six structural modes). Slight improvement in the performance was noted as n_c was increased, with about 15% improvement for n_c=9. Thus controlling more than the first 4 or 5 modes appears to contribute little towards the first objective (i.e., speed of response). However, since the damping ratios of the residual modes remain close to 0.01, the speed of response may not be satisfactory if the number of modes controlled is too small.

CONCLUDING REMARKS

Control systems synthesis was considered for a large flexible space antenna using two approaches. From the results based on the preliminary model and linear analysis, it appears that the performance requirements can be satisfactorily met, and an acceptable degree of stability and robustness can be obtained using either of the controllers. However, the LQG approach yielded much lower RMS errors, with significantly lower feedback gains. In addition, satisfactory performance was obtained with the LQG controller using as few as two actuators. Therefore, the LQG approach is more desirable for this problem. A method was given for generating parametrized performance data which would be useful as a design guideline. In order to arrive at more complete conclusions, however, it will be necessary to include the effects of actuator/sensor dynamics and nonlinearities. This can be accomplished only after the actuator concepts are selected and their characteristics known. It will also be useful to investigate other types of actuator concepts (e.g. reaction jets) prior to arriving at a control system design. Before commencing the final design process, it will also be necessary to precisely define the design objectives such as the speed of response requirement.

REFERENCES

1. Russell, R. A., Campbell, T. G., and Freeland, R. E.: A Technology Development Program for Large Space Antennas. NASA TM 81902, September, 1980.

2. Sullivan, M. R.: LSST (Hoop/Column) Maypole Antenna Development Program, Parts I and II. NASA CR 3558, June 1982.

3. Joshi, S. M.: A controller Design Approach for Large Flexible Space Structures. NASA CR 165717, May 1981.

4. Elliott, L. E., Mingori, D. L., and Iwens, R. P.: Performance of Robust Output Feedback Controller for Flexible Spacecraft. Proc. Second VPISU/AIAA Symposium on Dyanamics and Control of Large Flexible Spacecraft, Blacksburg, VA, June 1979, pp. 409-420.

5. Joshi, S. M.: Design of Stable Feedback Controllers for Large Space Structures. Proc. Third VPISU/AIAA Symposium on Dynamics and Control of Large Flexible Spacecraft, Blacksburg, VA, June 1981, pp. 527-539.

6. Aubrun, J. N., Lyons, M., Margulies, G., Arbel, A., and Gupte, N.: Stability Augmentation for Flexible Space Structures. 18th IEEE Conference on Decision and Control, Ft. Lauderdale, Florida, December 1979.

7. Balas, M. J.: Feedback Control of Flexible Systems. IEEE Trans. Automatic Control, Vol. 23, No. 4, August 1978, pp. 673-679.

8. Joshi, S. M., and Groom, N. J.: Controller Design Approaches for Large Space Structures Using LQG Control Theory. Proc. Second VPISU/AIAA Symposium on Dynamics and Control of Large Flexible Spacecraft, Blacksburg, VA, June 1979, pp. 35-50.

9. Sesak, J. R., Likins, P. W., and Coradetti, T.: Flexibl Spacecraft Control by Model Error Sensitivity Suppression (MESS). J. Astronautical Sciences, Vol. 27, No. 2, April-June 1979, pp. 131-156.

10. Joshi, S. M., and Groom, N. J.: Stability Bounds for the Control of Large Space Structures. AIAA J. Guidance and Control, Vol. 2, No. 4, July-August, 1979, pp. 349-351.

11. Joshi, S. M., and Groom, N. J.: A Two-Level Controller Design Approach for Large Space Structures. Proc., 1980 Joint Automatic Control Conference, San Francisco, CA, August, 1980.

12. Joshi, S. M.: On Attitude Estimation Schemes for Fine-Pointing Control. IEEE Trans. Aerospace and Electronic Systems, Vol. 14, No. 2, March 1978, pp. 258-265.

13. Smith, P. G.: Numerical Solution of the Matrix Equation $AX+XA^T+B=0$.
    IEEE Trans. Automatic Control, Vol. 16, No. 3, June 1971, pp. 278–
    279.

TABLE I. MASS AND INERTIA PROPERTIES

Mass= 4544.3 Kg.

Inertia about axes through center of mass $(Kg-m^2)$

$$I_{xx}= 5.724 \times 10^6 \qquad I_{yy}= 5.747 \times 10^6$$

$$I_{zz}= 4.383 \times 10^6 \qquad I_{xz}= 3.906 \times 10^4$$

$$I_{xy}= I_{yz}= 0$$

TABLE II. STRUCTURAL MODE FREQUENCIES

Mode no.	1	2	3	4	5	6	7	8	9	10
Freq. rad/sec	0.75	1.35	1.70	3.18	4.53	5.59	5.78	6.84	7.4	8.78

Mode no.	11	12	13	14	15	16	17	18	19	20
Freq. rad/sec	10.85	11.24	15.05	15.4	15.75	15.85	16.04	18.84	18.84	18.99
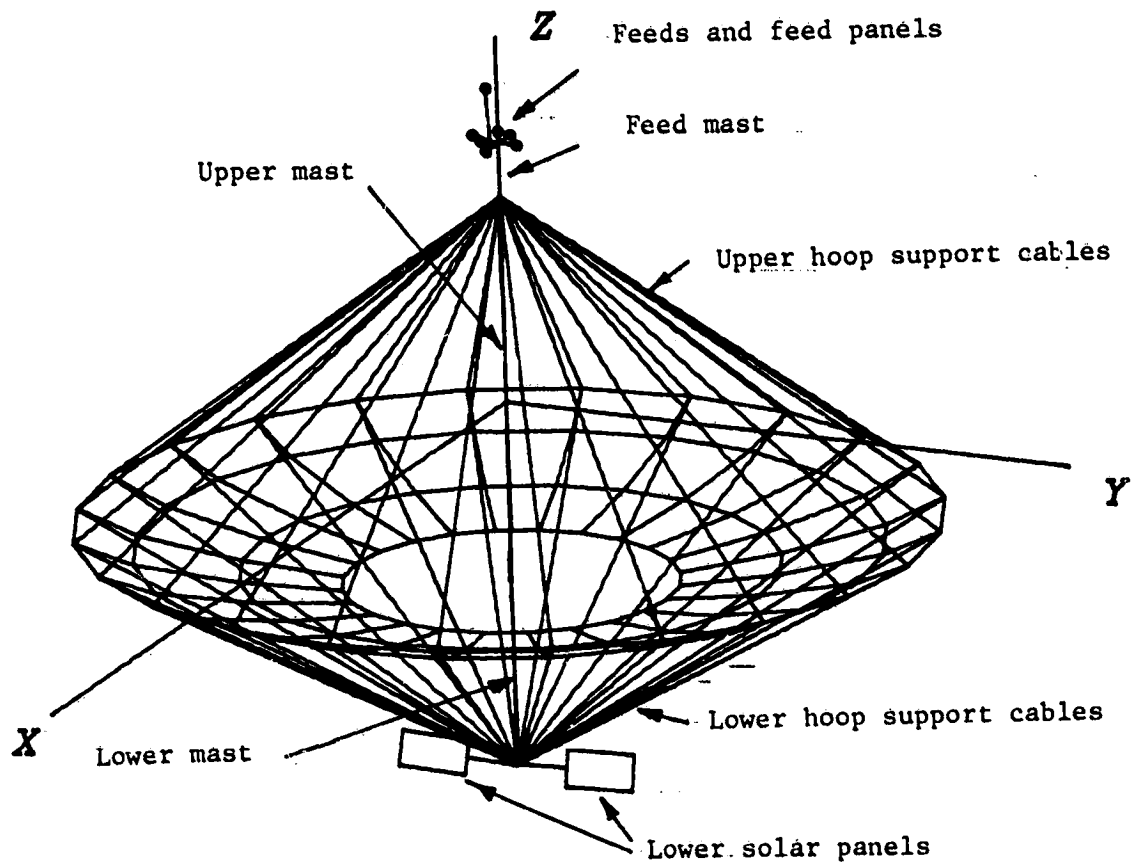
Figure 1. Hoop/column antenna concept

18
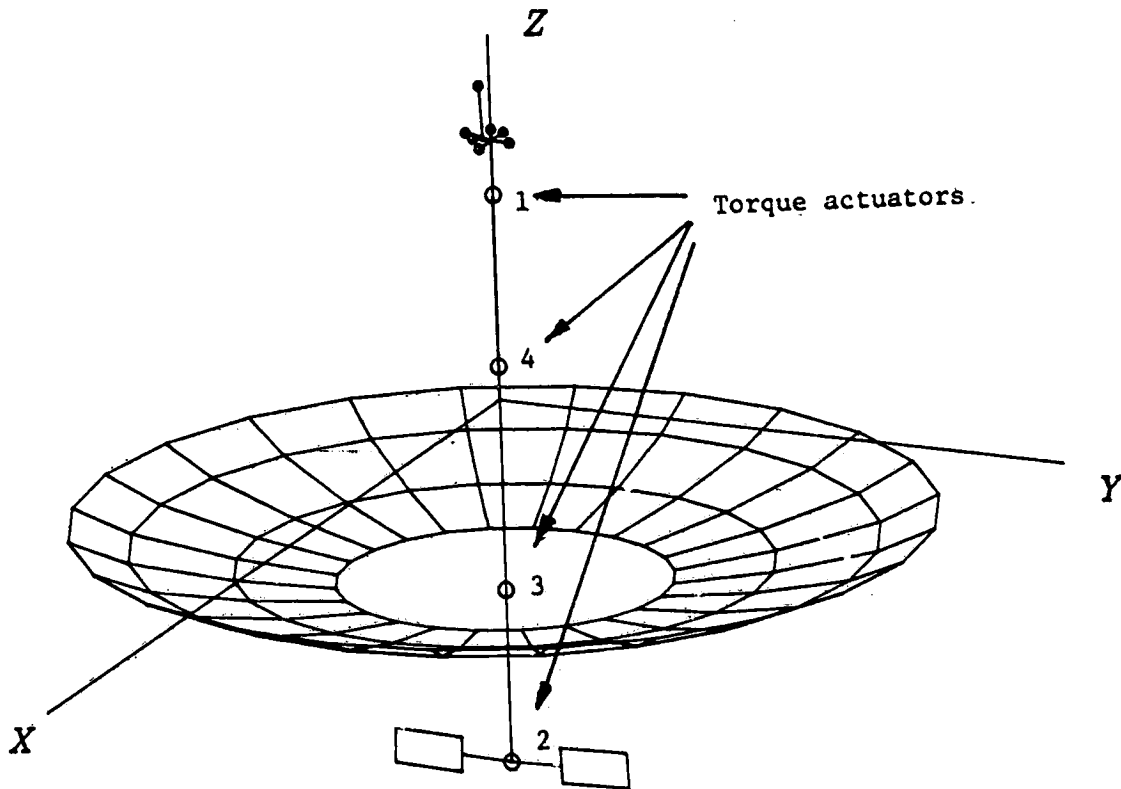
Figure 2. Assumed actuator locations
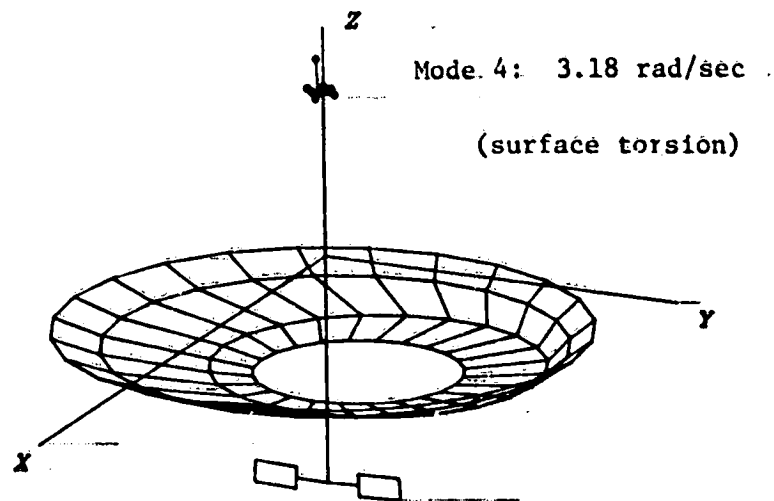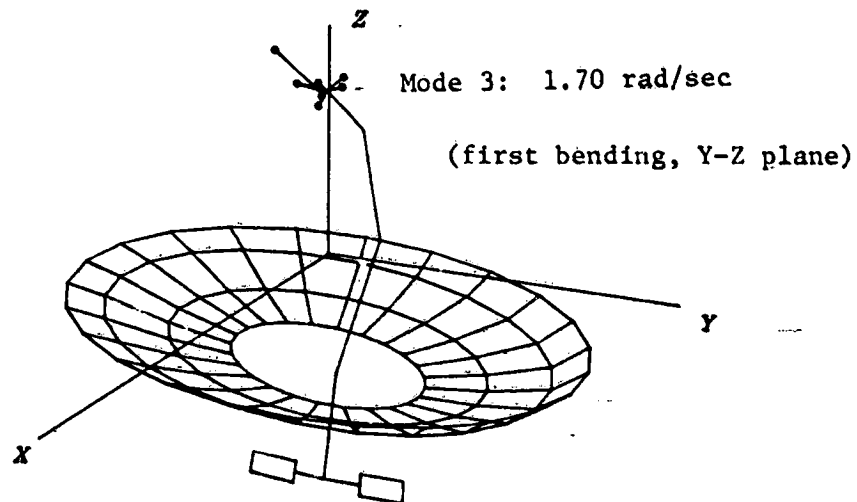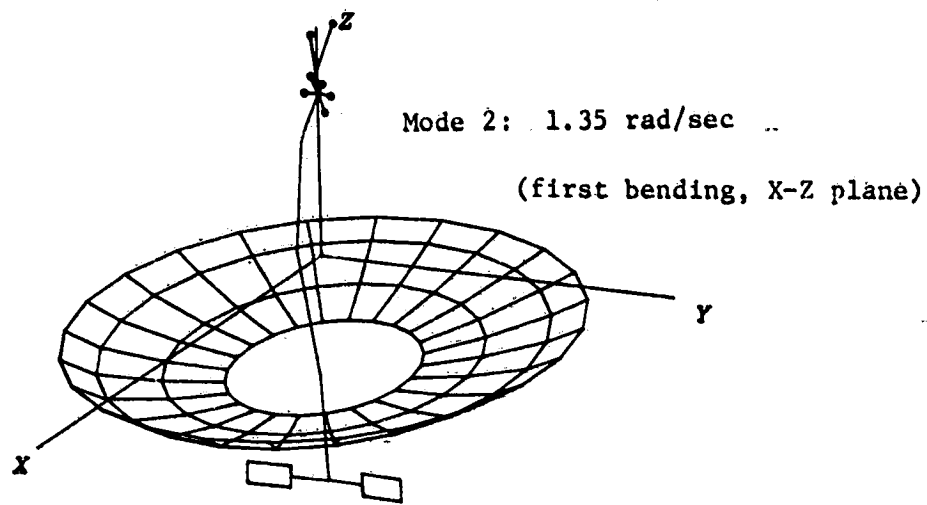
Mode 2: 1.35 rad/sec

(first bending, X-Z plane)

Mode 3: 1.70 rad/sec

(first bending, Y-Z plane)

Mode 4: 3.18 rad/sec

(surface torsion)

Figure 3. Plots of typical antenna mode-shapes

Mode 5: 4.53 rad/sec

(second bending, Y-Z plane)

Mode 7: 5.78 rad/sec

(second bending, X-Z plane)

Mode 8: 6.84 rad/sec
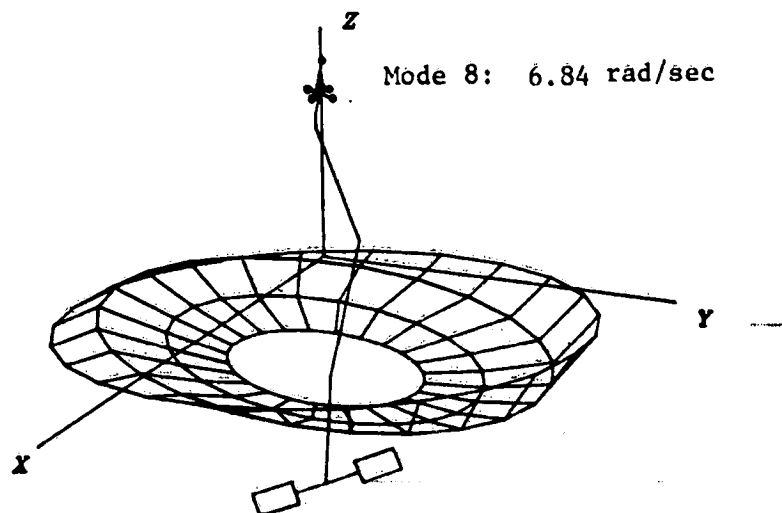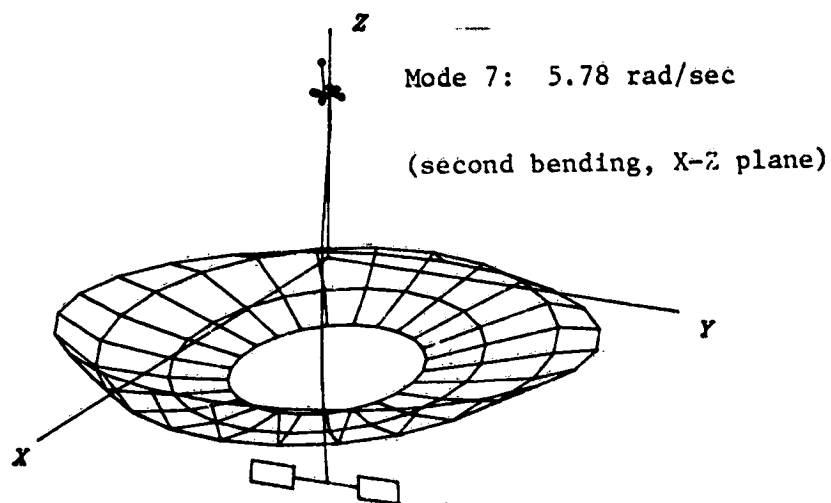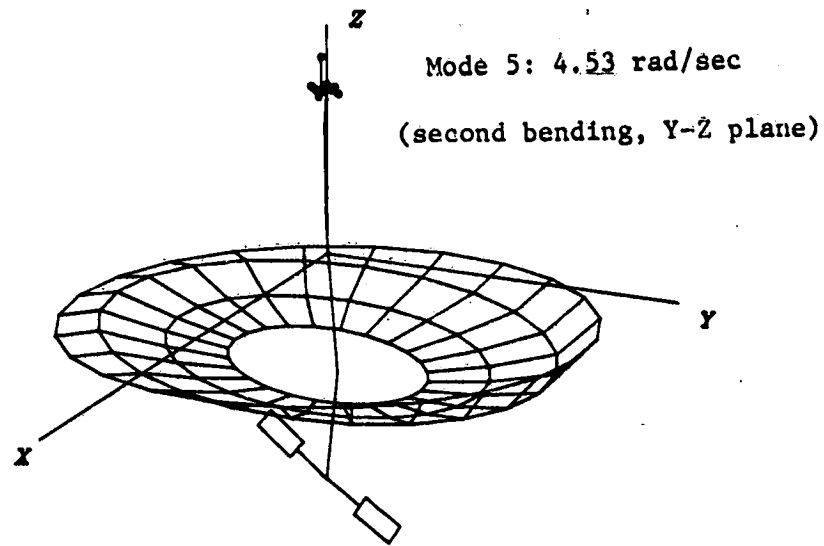
Figure 3.   Plots of typical antenna mode-shapes (Cont.)

21

Mode 9: 7.40 rad/sec.

Mode 10: 8.78 rad/sec
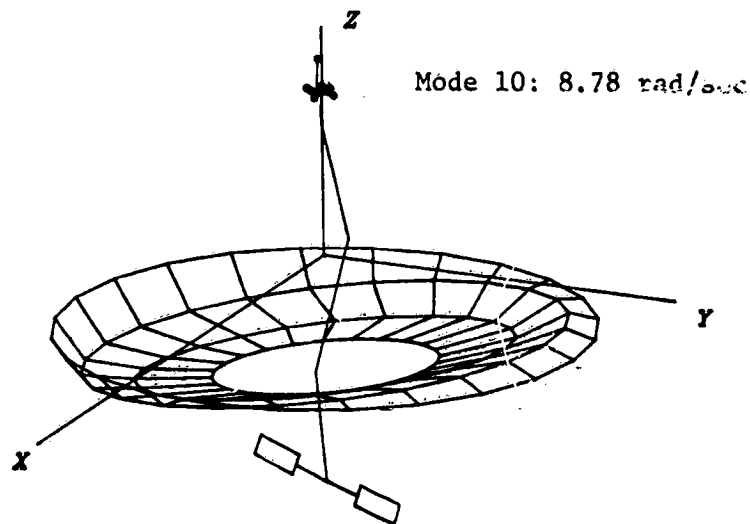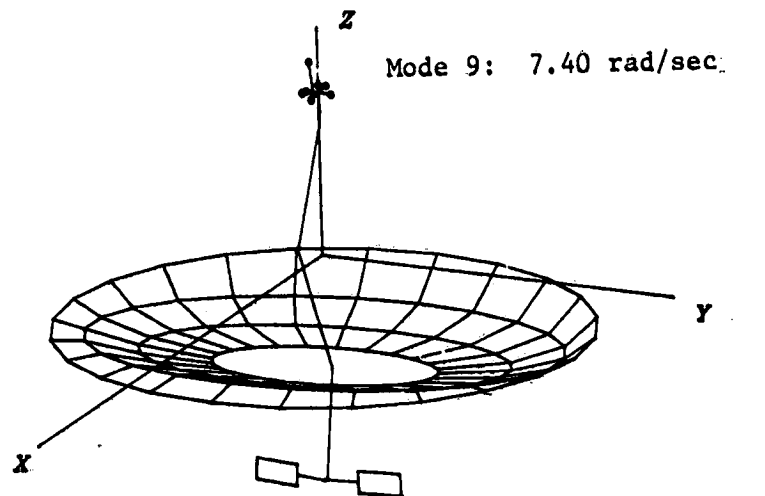
Figure 3. Plots of typical antenna mode-shapes (concluded)
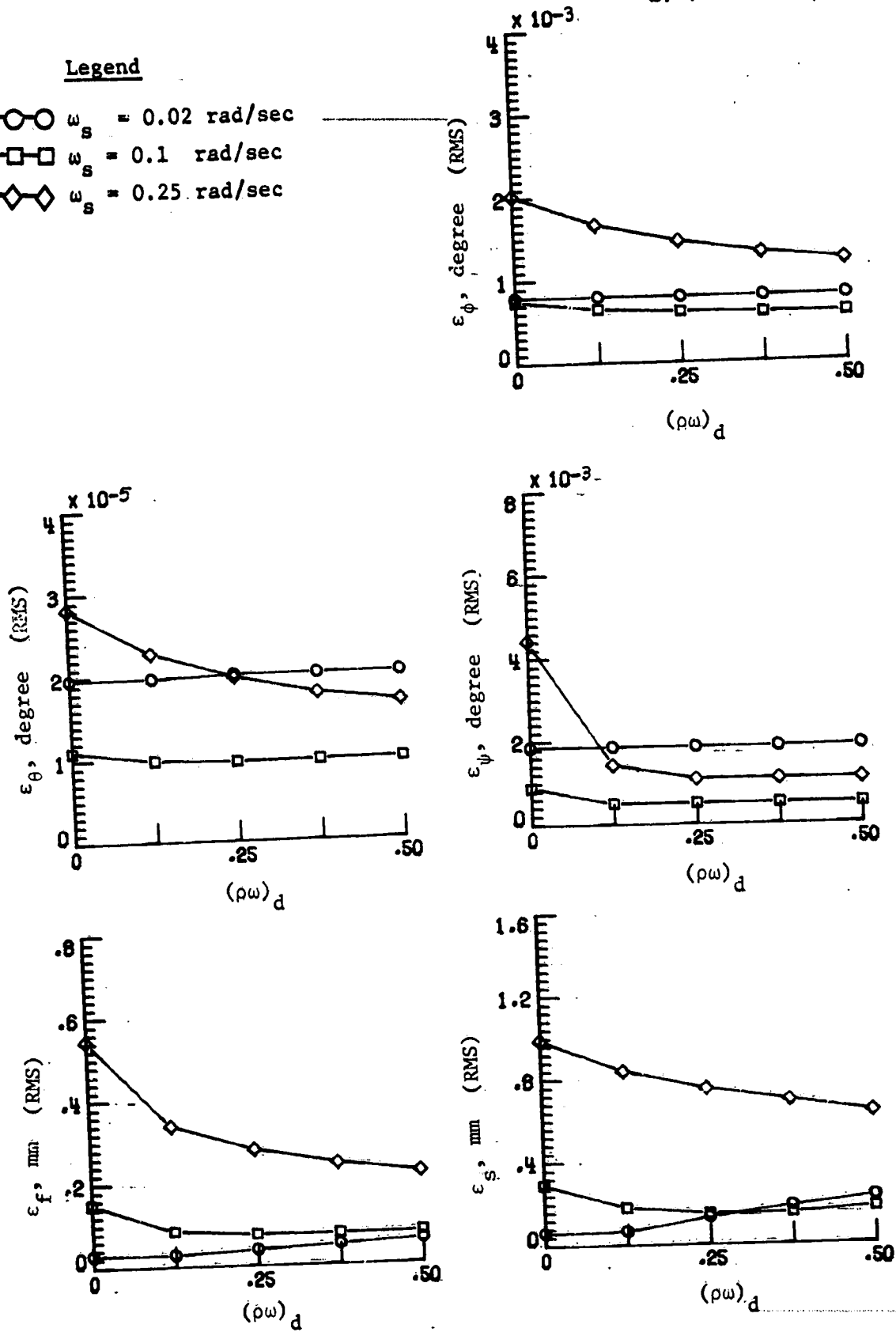
Figure 4. Performance of collocated controller
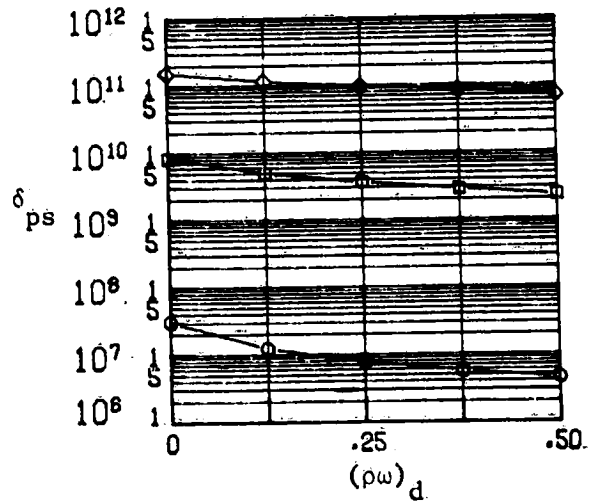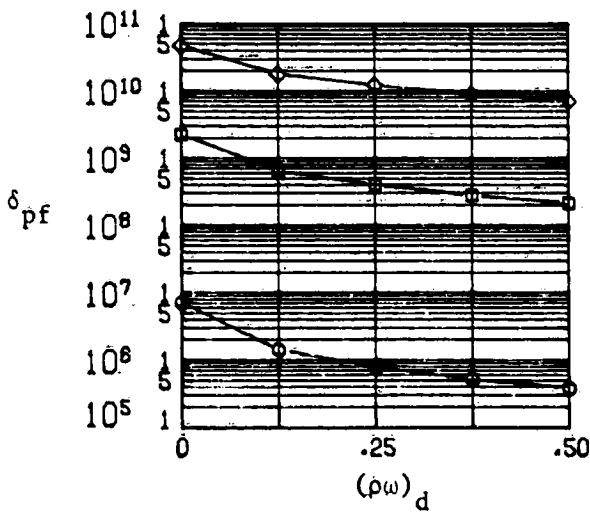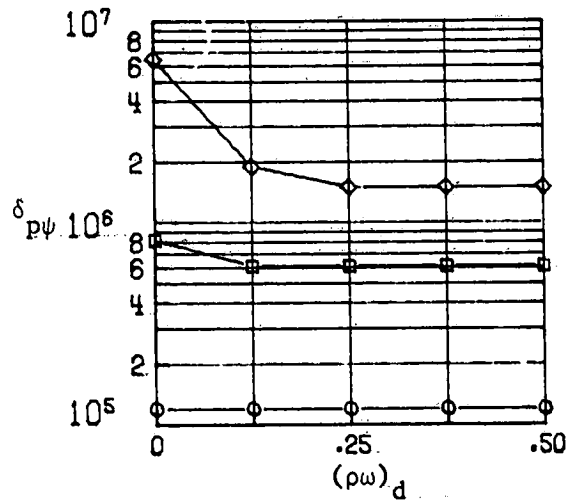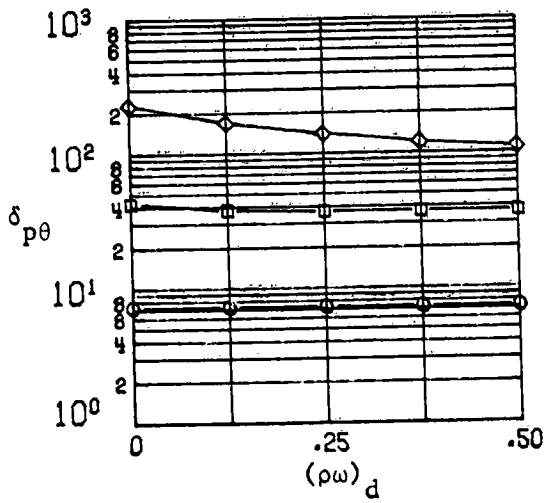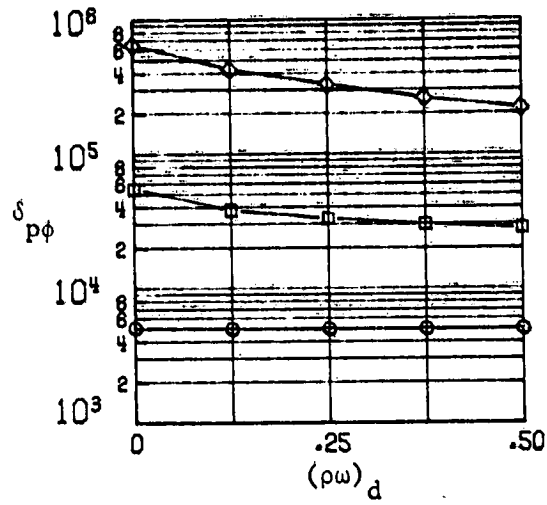
Figure 5. Collocated controller performance coefficients δ_p
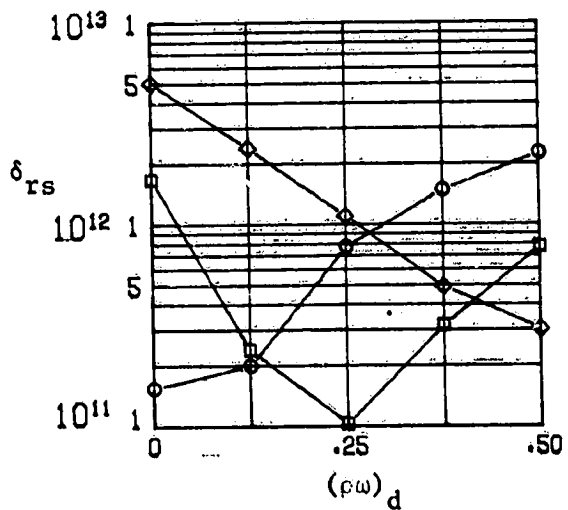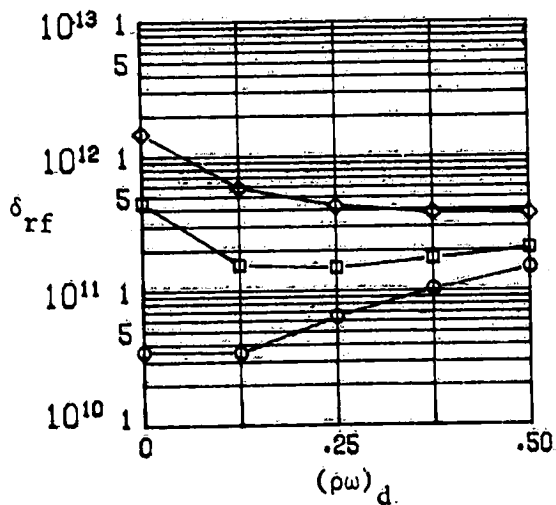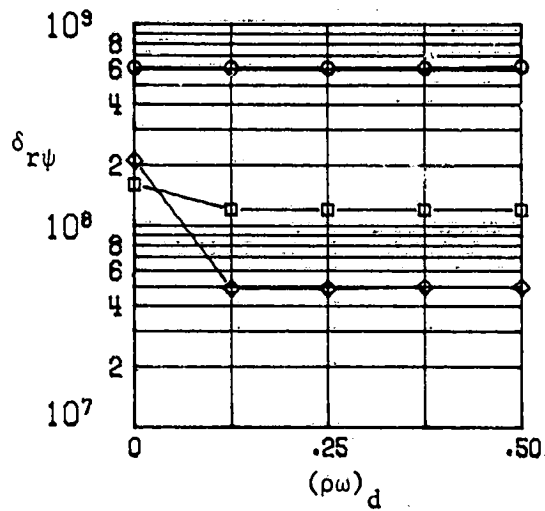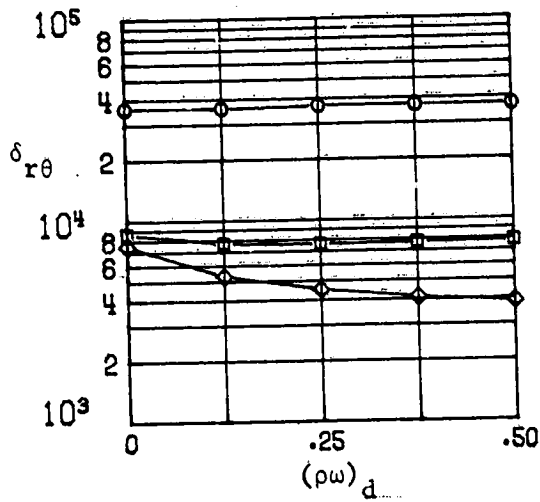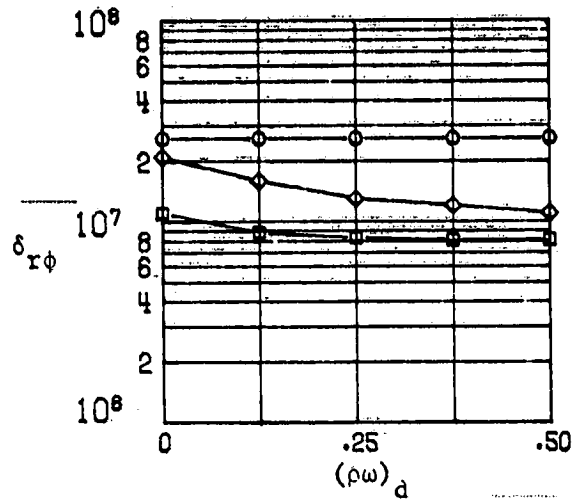
Figure 6. Collocated controller performance coefficients δ_r

25
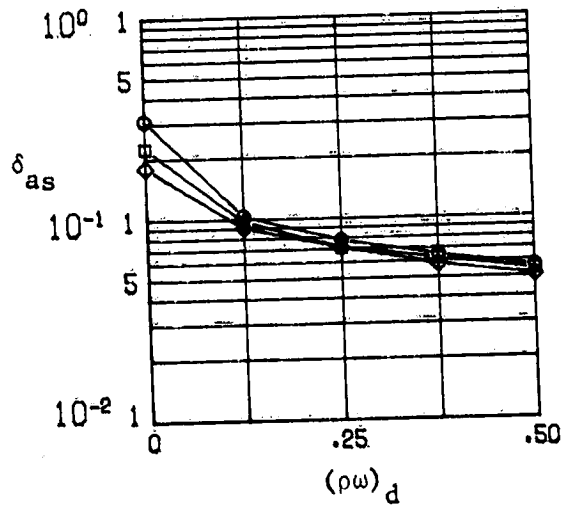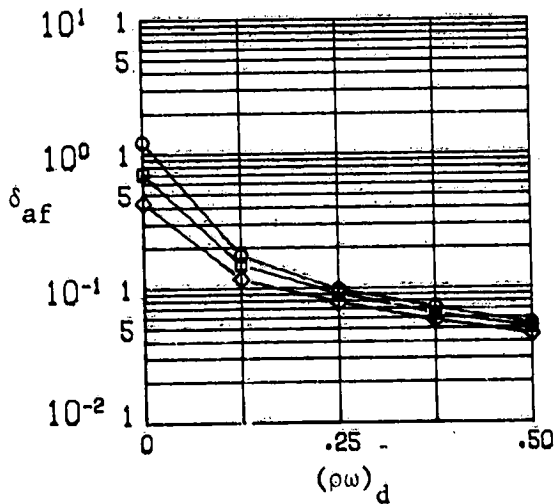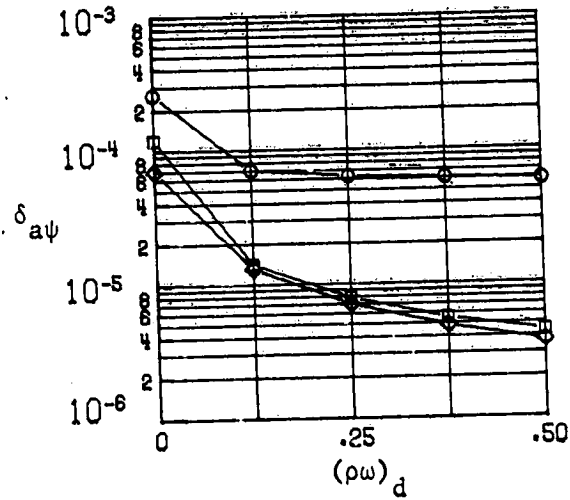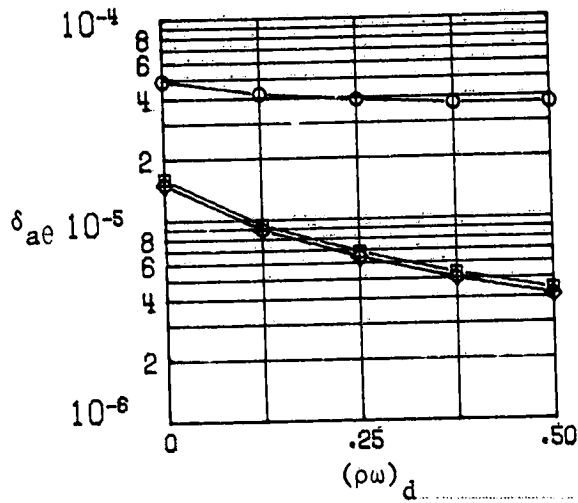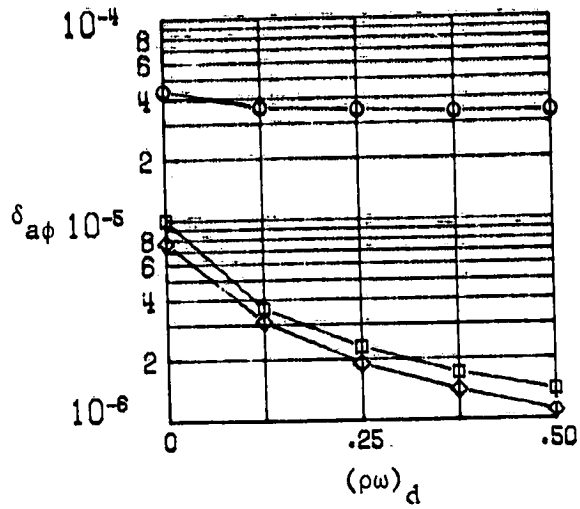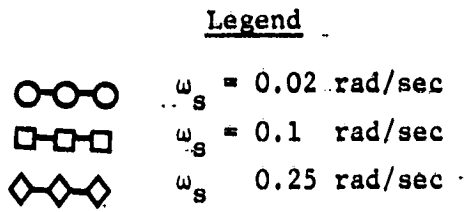
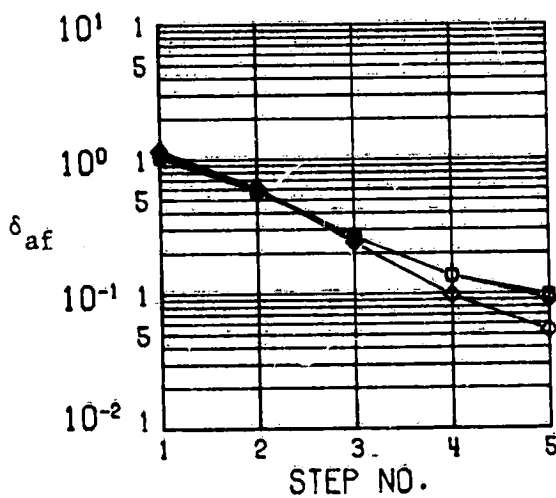Figure 7. Collocated controller performance coefficients δ_a
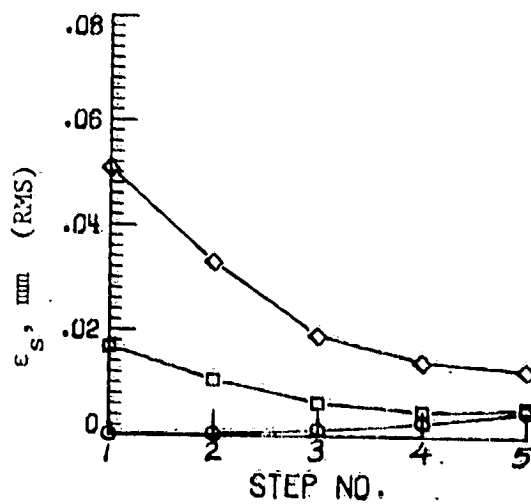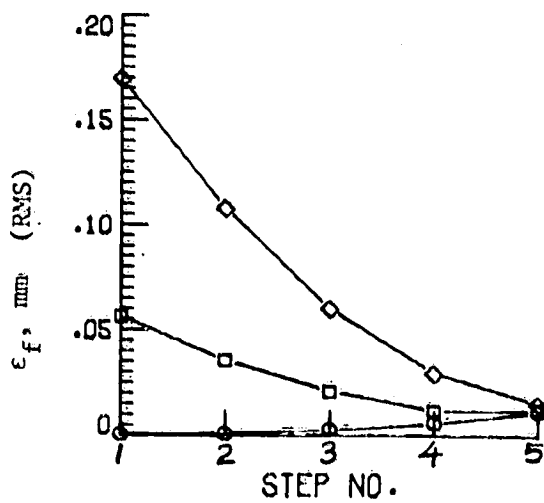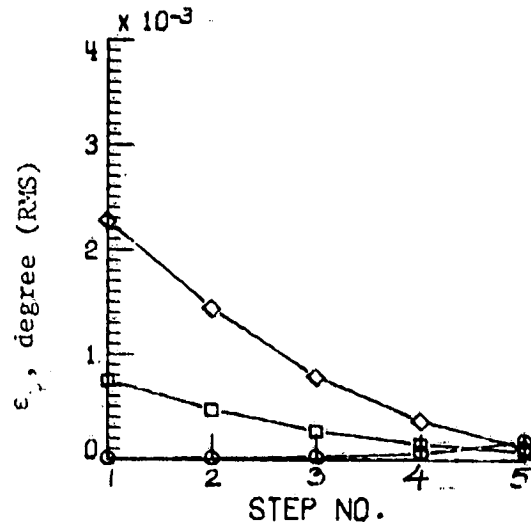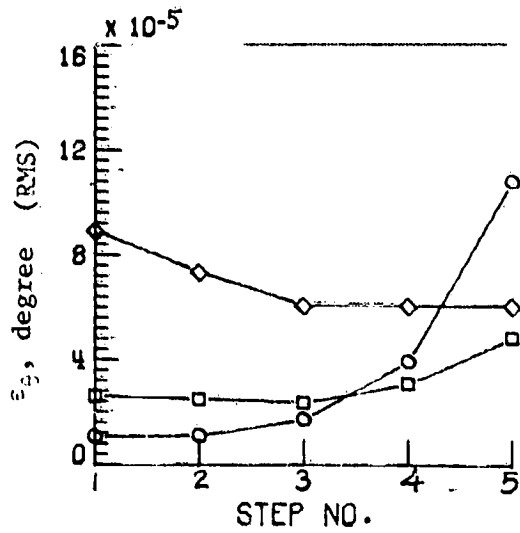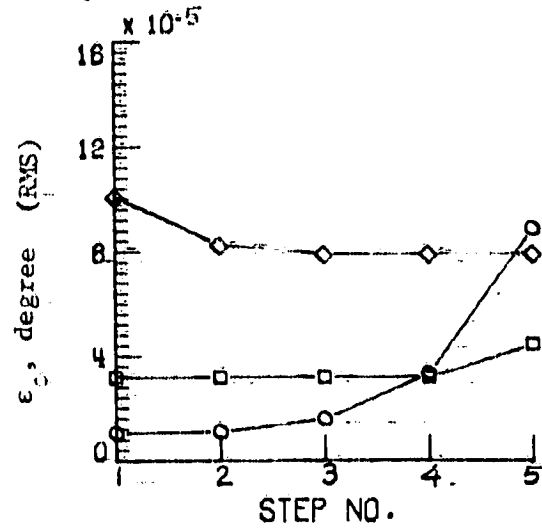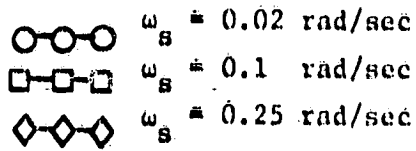
Figure 8. Performance of LQG controller
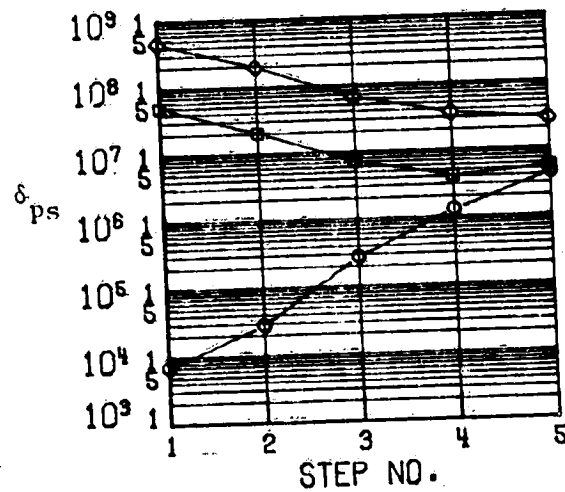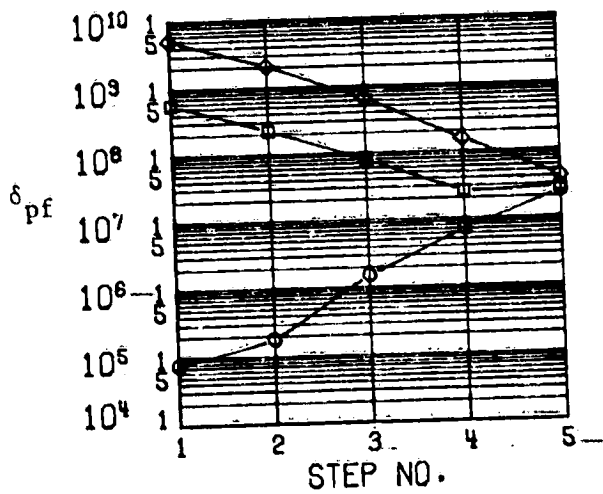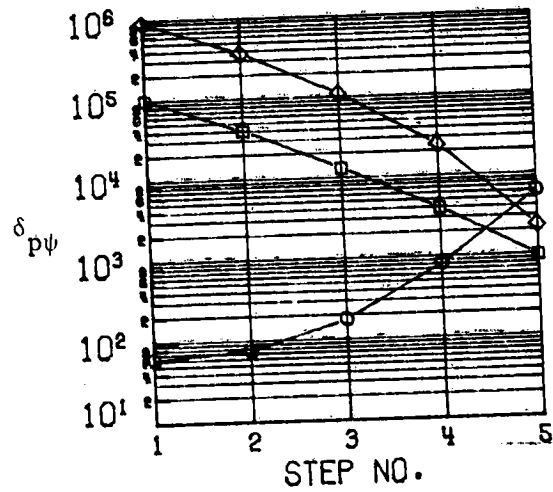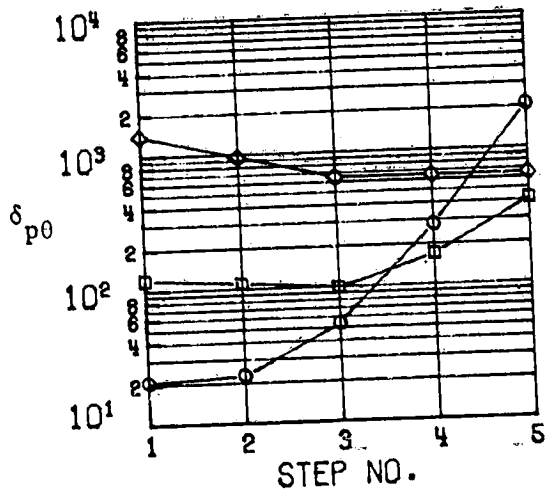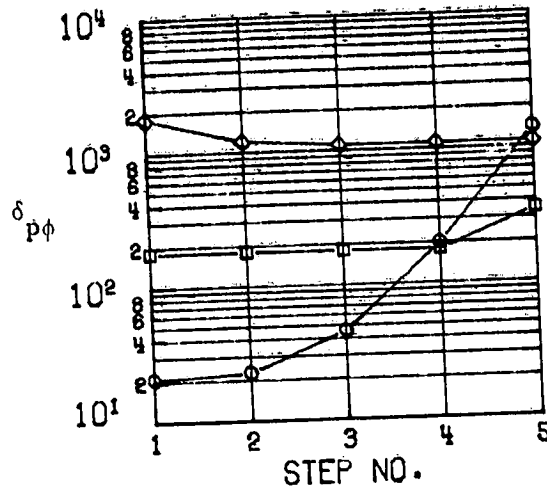
Figure 9. LQG controller performance coefficients δ_p
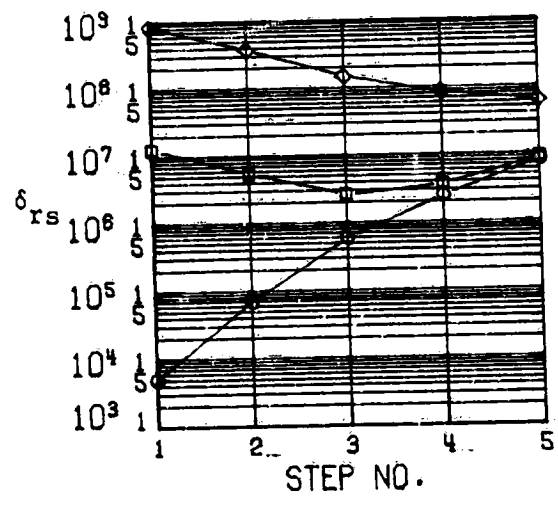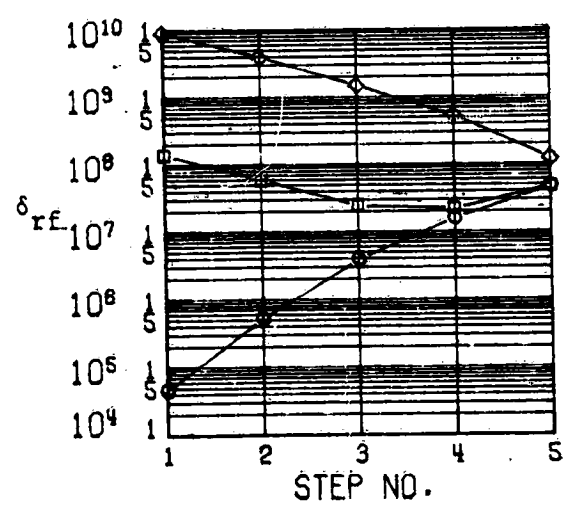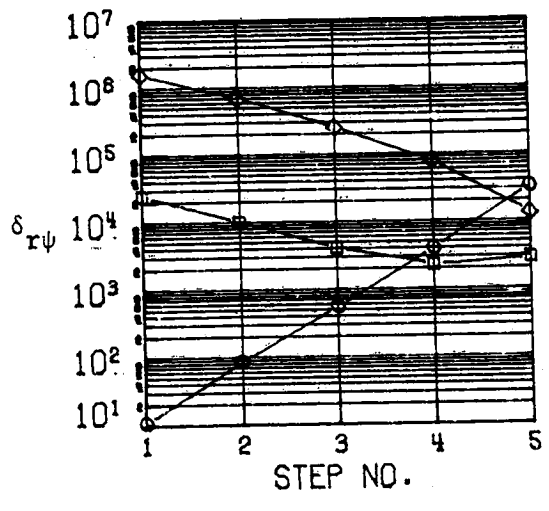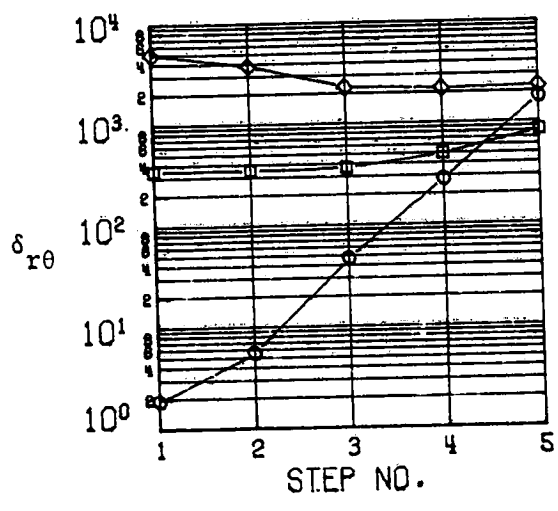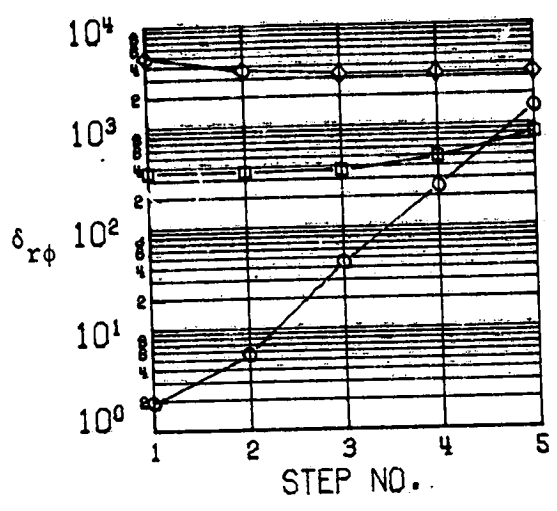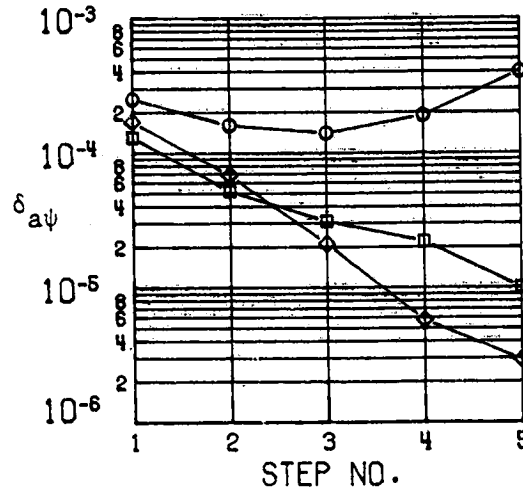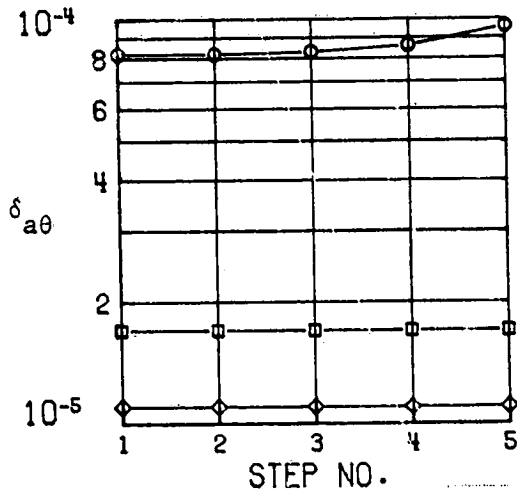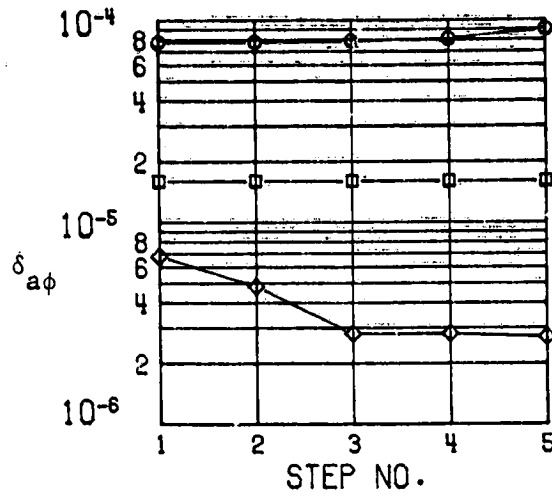
Figure 10. LQG controller performance coefficients δ_r
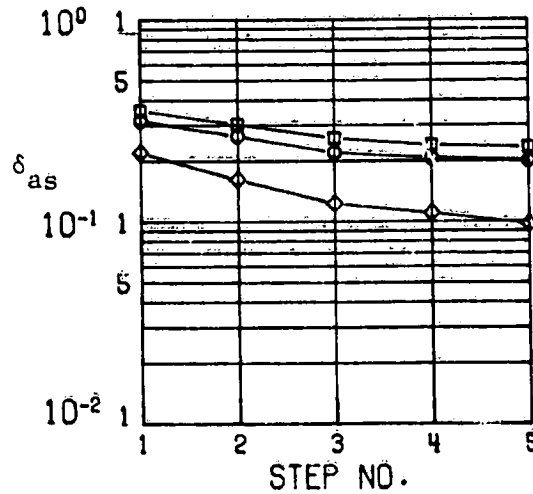
Figure 11. LQG controller performance coefficients δ_a